



Cite this: DOI: 10.1039/d1gc00374g

Received 1st February 2021.

Accepted 16th April 2021

DOI: 10.1039/d1gc00374g

rsc.li/greenchem

## Visible light induced hydrophosphinylation of unactivated alkenes catalyzed by salicylaldehyde†

Zeqin Yuan, Simin Wang, Miaomiao Li, Tian Chen, Jiaye Fan, Fuying Xiong, Qianggen Li, Ping Hu, Bi-Qin Wang, Peng Cao and Yang Li \*

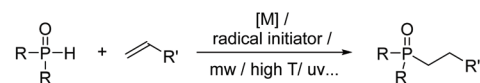
**An air and water insensitive visible light induced hydrophosphinylation of unactivated alkenes is reported. A small amount of a simple and cheap compound, salicylaldehyde, is used as a photosensitizer. The reaction is carried out in a basic aqueous solution which enables the deprotonated salicylaldehyde to show visible light absorption.**

Phosphorus containing organic compounds are of great importance owing to their unique functional activities. They have wide applications in the fields of medicine, agriculture, materials science and catalysis.<sup>1</sup> One of the most important strategies for the construction of organophosphorus compounds relies on C–P bond formation through transition metal mediated coupling, nucleophilic substitution, addition reaction and so on.<sup>2</sup> Among them, the hydrophosphinylation of unsaturated bonds represents one of the simple, efficient and atom-economical approaches for the synthesis of novel tertiary phosphine oxides.<sup>3</sup> Reactions with unactivated alkene substrates are difficult to carry out because they require transition metals,<sup>4</sup> radical initiators,<sup>5</sup> mw,<sup>6</sup> high temperature,<sup>4–7</sup> or UV light<sup>8</sup> for activation (Scheme 1a).

In recent years, visible light induced photocatalysis has become a powerful strategy which renders the reaction conditions greener and milder.<sup>9</sup> This strategy has also been successfully applied in the synthesis of organophosphorus compounds through C–P bond formation.<sup>10</sup> In 2013, Kobayashi reported an elegant hydrophosphinylation of unactivated alkenes induced by visible light.<sup>10a,11</sup> This reaction proceeded exceedingly well when an iridium complex was used as the catalyst in the initial study, and the author managed to replace the metal complex with the organic dye Rhodamine B with an

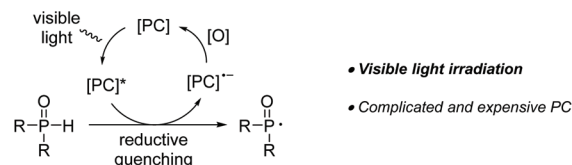
equivalent catalytic ability. The mechanism involves the generation of a phosphonyl radical directly through reductive quenching from the photoredox catalytic cycle (Scheme 1b; photocatalyst: PC).<sup>9a–c,g,i</sup> Inspired by this work, the phosphonyl radical addition across unsaturated substrates was expanded to the hydrophosphinylation of alkynes,<sup>12</sup> oxidative phosphorylation,<sup>13</sup> cascade phosphoryl radical cyclization,<sup>14</sup> oxyphosphorylation,<sup>11,15</sup> migratory carbophosphinylation<sup>16</sup> and phosphonocarboxylation.<sup>17</sup> In these reactions, noble

### (a) Hydrophosphinylation of unactivated alkenes using traditional methods:



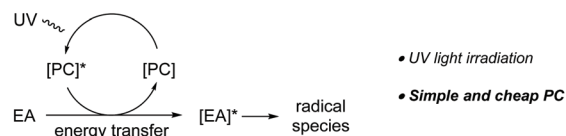
### (b) Visible light induced phosphoryl radical generation:

Representative photoredox process:

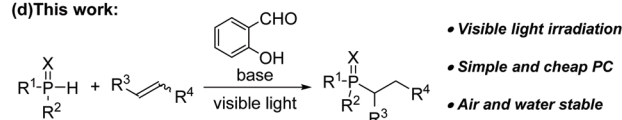


### (c) Simple aldehyde catalyzed photoinduced reaction:

Representative energy transfer process:



### (d) This work:



Scheme 1 Reaction design.

College of Chemistry and Materials Science, Sichuan Normal University, Chengdu 610068, China. E-mail: yangli@sicnu.edu.cn

† Electronic supplementary information (ESI) available: Experimental details, NMR spectra, light spectra and computational studies. See DOI: 10.1039/d1gc00374g

metal-based complexes or organic molecules with a relatively big  $\pi$ -conjugated ligand or a structural scaffold were commonly used as the catalyst (Scheme 1b).

To further reduce the cost of visible light induced reactions, simplifying the photocatalyst to smaller and cheaper organic compounds has received a lot of attention.<sup>9g,h,18</sup> In 2017, Mathé and coworkers used a simple aromatic ketone, 2,2-dimethoxy-2-phenylacetophenone (DPAP), as a photoinitiator in P–H addition to unsaturated carbon–carbon bonds.<sup>8c</sup> However, higher energy light (UV-A, 365 nm, 60 W) was required for this reaction. Several examples show that simple aromatic aldehydes are able to catalyze addition reactions to alkenes under light irradiation.<sup>19</sup> A representative mechanism includes an energy transfer (EnT) process<sup>9i–l</sup> from the excited state catalyst to the substrate (energy acceptor: EA), following the generation of reactive radical species (Scheme 1c).<sup>19a,c</sup> Again, due to the nature of the small  $\pi$ -conjugated system of these simple catalysts, high energy of light activation is often needed (mainly in the UV region).<sup>20</sup> Last year, Kang and coworkers presented a visible light induced reaction catalyzed by salicylaldehyde.<sup>21</sup> The authors discovered that the light absorption of salicylaldehyde in DMSO solution shows a red shift from 324 to 417 nm when deprotonated by  $K_3PO_4$ . A visible light induced EnT process was shown to activate the corresponding substrates (Scheme 1c). We were interested in exploring versatile C–P coupling reactions, and we envisioned that this strategy could be used to trigger phosphonyl radical additions across alkenes. Herein, we report an air insensitive and visible light induced hydrophosphinylation of unactivated alkenes in a salicylaldehyde-base aqueous solution (Scheme 1d).

As shown in Table 1, diphenylphosphine oxide **1a** (0.1 mmol) and 1-hexene **2a** (2.0 equivalent) were chosen as standard substrates. They reacted smoothly in the presence of 2.5 mol% salicylaldehyde, 2.5 equivalents  $Na_2CO_3$  in  $H_2O$  under air atmosphere and irradiation with 30 W blue LEDs.<sup>22</sup> The NMR yield reached 95% after overnight reaction (Table 1, entry 1). It was later found that the reaction reached completion after 3 hours. Control experiments showed that the presence of the catalyst, base and blue LED is indispensable (Table 1, entries 2–5). These satisfactory results were further improved when the reaction was carried out under an argon atmosphere with degassed  $H_2O$ , although extra experimental complications were introduced (Table 1, entry 6). When the reaction was carried out under an oxygen atmosphere and with oxygen saturated  $H_2O$ , the NMR yield decreased to 69% (Table 1, entry 7). Benzaldehyde was not able to promote this reaction (Table 1, entry 8). Changing the position of substitution of the hydroxyl group on the catalyst reduced the catalytic ability (Table 1, entries 9 and 10). Other organo-photocatalysts were also tested to replace salicylaldehyde. The commonly used organic dye Solvent Red 43 promoted the reaction and gave the product in 68% NMR yield (Table 1, entry 11). DPAP showed a much lower catalytic ability under the standard reaction conditions (Table 1, entry 12).<sup>8c</sup> Pyridoxal phosphate (PLP), a co-factor of the vitamin B6 family, contains an

Table 1 Screening results<sup>a</sup>

cat. 2

cat. 3

cat. 4

cat. 5 Solvent Red 43

cat. 6 DPAP

cat. 7 Pyridoxal Hydrochloride

Entry	Deviation from the standard conditions	NMR yield <sup>b</sup>
1	None	95%
2	No cat. 1	<5%
3	No $Na_2CO_3$	7%
4	No blue LED	NR
5	No blue LED, 60 °C	NR
6	Under Ar	>99%
7	Under $O_2$	69%
8	Cat. 2 instead of cat. 1	<5%
9	Cat. 3 instead of cat. 1	47%
10	Cat. 4 instead of cat. 1	24%
11	Cat. 5 instead of cat. 1	68%
12	Cat. 6 instead of cat. 1	30%
13	Cat. 7 instead of cat. 1	66%
14	$Ru(bpy)_3Cl_2 \cdot 6H_2O$ instead of cat. 1	52%
15	$Ir(ppy)_2(bpy) \cdot BF_4$ instead of cat. 1	95%

<sup>a</sup> All reactions were performed using **1a** (0.1 mmol), **2a** (0.2 mmol), 2.5 mol% catalyst, 2.5 equivalent  $Na_2CO_3$  and 0.1 mL distilled  $H_2O$  under 30 W blue LED irradiation under an air atmosphere overnight (20–24 hours). <sup>b</sup> Determined by crude  $^1H$  NMR using 1,2-dichloroethane ( $ClCH_2CH_2Cl$ ) as an internal standard.

*ortho*-hydroxyl substituted heteroaromatic aldehyde core structure.<sup>23</sup> We tested its derivative pyridoxal hydrochloride in this reaction, and the product was generated in 66% NMR yield (Table 1, entry 13). Metal based photoredox catalysts were also active under these reaction conditions (Table 1, entries 14 and 15), and  $Ir(ppy)_2(bpy) \cdot BF_4$  showed comparative results to salicylaldehyde.

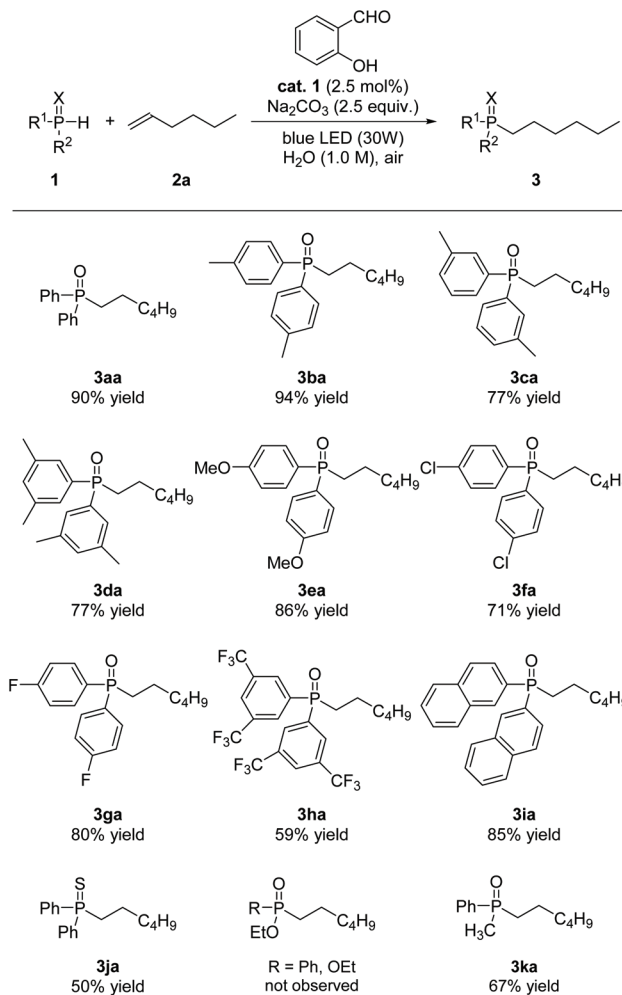
For a better understanding of the function of salicylaldehyde, we measured the UV-visible absorption spectra of the aldehyde catalysts **cat. 1–4** and **cat. 7** (see the ESI† for details). Without any base, these catalysts show no absorption in the visible light region. In the presence of  $Na_2CO_3$  (100 times compared to the aldehyde catalyst, the same ratio as under the standard reaction conditions), **cat. 1** shows the best red-shift absorption in the  $\lambda > 400$  nm region. The spectral irradiance of the blue LED was tested. It shows a light distribution that starts from 400 nm ( $\lambda_{max} = 459$  nm) and is in accordance with the visible light absorption of the catalysts. Under the standard

reaction conditions, the product was generated in 56% NMR yield after 1 hour and the yield was not increased (stirred overnight) after the irradiation was stopped. This observation indicates that visible light is required for the whole reaction process.

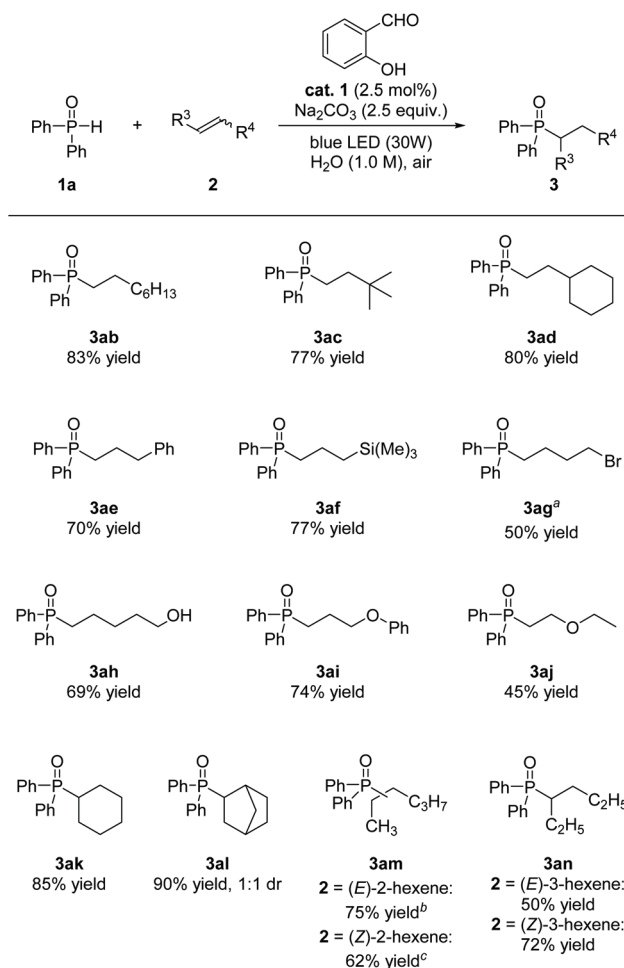
With the best reaction conditions in hand, the scope of the secondary phosphine oxide (SPO) was evaluated (Scheme 2). Using the standard substrate, the product **3aa** was isolated in 90% yield. Following this good result, both electron-rich and -poor SPOs reacted smoothly and produced the products in generally high yields. Di-*p*-tolylphosphine oxide gave **3ba** in 94% yield. Di-*m*-tolylphosphine oxide and bis(3,5-dimethylphenyl)phosphine oxide showed similar reactivities, giving both the corresponding products in 77% yield (**3ca** and **3da**). Di-*o*-tolylphosphine oxide was also tested. However, no reactivity was observed. This might be due to the negative steric effect on the P radical generation. The more electron rich diphenylphosphine oxide with the methoxyl substituent provided **3ea** in 86% yield. When electron poor diphenyl-

phosphine oxide with a *para* Cl- or F-substituent was used, **3fa** and **3ga** were obtained in 71% and 80% yields. Using bis(3,5-bis(trifluoromethyl)phenyl)phosphine oxide, the product **3ha** was generated in lower yield. An SPO with a bigger  $\pi$ -system such as di(2-naphthalenyl)phosphine oxide reacted smoothly under these reaction conditions and the product **3ia** was obtained in high yield (85%). Secondary phosphine sulfide was shown to be compatible in this reaction, despite a lower yield of the product being obtained (**3ja**, 50% yield). Hydrophosphorylation with ethyl phenylphosphinate or diethyl phosphonate was unsuccessful under these reaction conditions. To our delight, high reactivity was observed when methyl(phenyl)phosphine oxide was used, affording **3ka** in 67% yield.<sup>3e,24</sup>

Next, a variety of unactivated alkenes were evaluated by reacting with diphenylphosphine oxide **1a** (Scheme 3). More aliphatic external alkenes were tested, and the products were



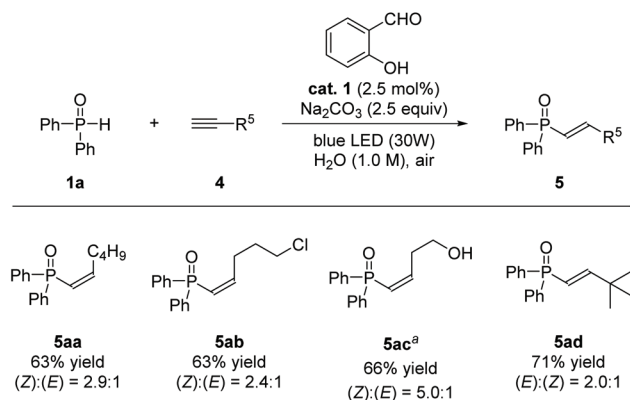
**Scheme 2** The scope of secondary phosphine oxides. Reaction conditions: **1** (0.2 mmol), **2a** (0.4 mmol), **cat. 1** (0.005 mmol),  $\text{Na}_2\text{CO}_3$  (0.5 mmol), distilled  $\text{H}_2\text{O}$  (0.2 mL), 30 W blue LED, air atmosphere.



**Scheme 3** The scope of unactivated alkenes. Reaction conditions: **1a** (0.2 mmol), **2** (0.4 mmol), **cat. 1** (0.005 mmol),  $\text{Na}_2\text{CO}_3$  (0.5 mmol), distilled  $\text{H}_2\text{O}$  (0.2 mL), 30 W blue LED, air atmosphere. <sup>a</sup> 4.0 equivalents of the corresponding alkene are used. <sup>b</sup> Regioselectivity: hexan-2-ylidiphenylphosphine oxide/hexan-3-ylidiphenylphosphine oxide = 1.1:1. <sup>c</sup> Regioselectivity: hexan-2-ylidiphenylphosphine oxide/hexan-3-ylidiphenylphosphine oxide = 1.5:1.

generated in high yields (**3ab–3ad**). Functional groups such as phenyl and trimethylsilyl groups were tolerated under these reaction conditions (**3ae** and **3af**). It has been shown that SPO was able to undergo nucleophilic substitution with haloalkanes under basic reaction conditions.<sup>25</sup> We were happy to find out that substrates bearing a bromide group were also tolerated in this reaction, although a lower yield was obtained and no substituted side product was observed (**3ag**). Not much negative effect due to the base was observed when an alkene with a hydroxyl group was used, and the product **3ah** was generated in 69% yield. Two terminal alkenes with an ether group were examined. When allylic phenyl ether was used as the substrate, 74% yield of **3ai** was obtained. When active terminal alkene ethoxyethene was used, the reaction was able to generate the anti-Markovnikov adduct **3aj** in 45% yield. Cyclic internal alkenes showed high reactivities in this reaction, furnishing **3ak** and **3al** in 85% and 90% yield, respectively. Finally, linear internal alkenes were tested, and the alkenes with both (*E*)- and (*Z*)-configurations were able to undergo the reaction smoothly. In the case of (*E*)-2-hexene and (*Z*)-2-hexene, the product **3am** was obtained in 75% and 62% yield, respectively, although the regioselectivities were low. Using (*E*)-3-hexene and (*Z*)-3-hexene, **3an** was generated as a single isomer in 50% and 72% yield, respectively.

This methodology was expanded to unactivated terminal alkynes (Scheme 4). The alkynes with both linear and branched R<sup>5</sup> groups reacted well with **1a**, and substrates bearing chloro or hydroxyl substituents were tolerated. In the case of substrates where the R<sup>5</sup> group is less hindered, the adducted products were generated mainly in the (*Z*)-configuration, with the products **5aa**, **5ab** and **5ac** being obtained in good yields (63%, 63% and 66%) and with moderate (*Z*):(*E*) selectivities (2.9:1, 2.4:1 and 5:1). In the substrate with the bulky R<sup>5</sup> group (*t*-Bu), the product **5ad** was generated mainly in the (*E*)-configuration (2:1) in 71% yield. These results



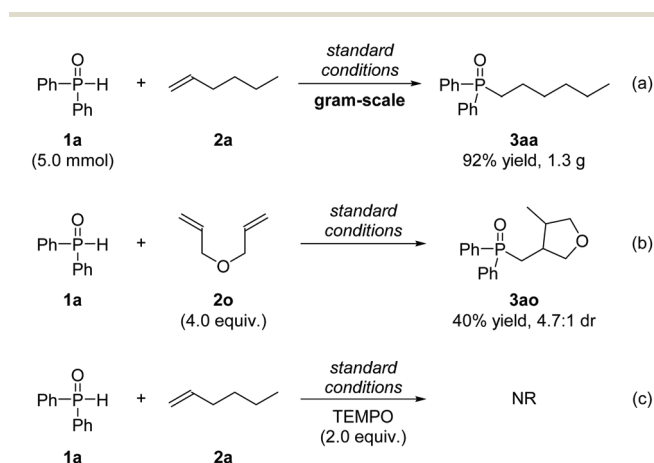
**Scheme 4** The scope of unactivated alkynes. Reaction conditions: **1a** (0.2 mmol), **4** (0.4 mmol), **cat. 1** (0.005 mmol), Na<sub>2</sub>CO<sub>3</sub> (0.5 mmol), distilled H<sub>2</sub>O (0.2 mL), 30 W blue LED, air atmosphere. Total yield of the (*Z*)- and (*E*)-configurations was reported. The (*Z*):(*E*) or (*E*):(*Z*) ratio was determined from the isolated yield. <sup>a</sup> The (*Z*):(*E*) ratio was determined by crude <sup>1</sup>H NMR.

might indicate that a phosphonyl radical addition mechanism is involved in the generation of vinyl radical intermediates.<sup>26</sup>

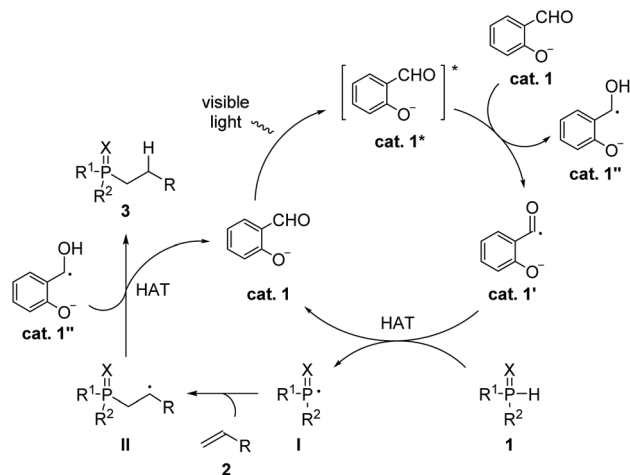
To further prove the utility of this method, a gram scale reaction was carried out (Scheme 5a). The reaction was easily scaled up to 5.0 mmol and performed well under the standard reaction conditions, with the product being obtained with slightly improved yield (92%). The reaction of SPO **1a** with diallyl ether **2o** was performed, affording the cyclic product **3ao** in 40% yield and 4.7:1 dr (Scheme 5b). The standard reaction was carried out in the presence of 2.0 equivalents of TEMPO and no reaction was observed (Scheme 5c). These results indicated that the reaction mechanism involves the generation of the phosphonyl radical species.

To explain the mechanism of phosphonyl radical generation, several possibilities were discussed. The cyclic voltammetric behavior of salicylaldehyde in buffers with differing pH values has been studied by He and coworkers.<sup>27</sup> According to this work we expect that the anodic peak potential of the catalyst under our standard reaction conditions (2.5 M Na<sub>2</sub>CO<sub>3</sub> solution, around 12.32 pH value) is approximately 0.995 V vs. SHE. The oxidative potential of **1a** could be estimated to be around 1.245 vs. SHE.<sup>10a,28</sup> The excited state of the deprotonated catalyst might not be able to oxidize **1a** to the phosphonyl radical (Scheme 1b).

The energy difference between the ground state and excited triplet state of the deprotonated salicylaldehyde was calculated ( $\Delta E = 54.7$  kcal mol<sup>-1</sup>), and it was lower than the calculated triplet energies of **1a** and its isomer hydroxydiphenylphosphane (**1a'**) ( $\Delta E = 85.0$  kcal mol<sup>-1</sup> and 65.6 kcal mol<sup>-1</sup>, respectively). The direct P–H and O–H bond dissociation energy values of **1a** and **1a'** were also calculated to be relatively high ( $\Delta E = 87.7$  kcal mol<sup>-1</sup> and 86.5 kcal mol<sup>-1</sup> respectively). On the other hand, there is no overlap of the fluorescence emission spectrum of deprotonated **cat. 1** and the absorption spectrum of **1a** (see the spectra in the ESI<sup>†</sup>). The absolute fluorescence quantum yield of deprotonated **cat. 1** is also relatively low.<sup>29</sup> All these results indicate that the phosphine oxide substrate could not be excited by the excited catalyst through EnT



**Scheme 5** Scale up reaction and radical trapping reactions.



Scheme 6 Mechanism proposal.

processes (neither the Dexter EnT process nor the fluorescence resonance EnT process)<sup>9i-1</sup> (Scheme 1c).

In 2019, Kokotos and coworkers published a photochemical hydroacylation of alkenes using 4-cyanobenzaldehyde as the photoinitiator.<sup>19b,e</sup> They proposed that the triplet state of 4-cyanobenzaldehyde interacts with a ground state molecule of 4-cyanobenzaldehyde and generates a benzoyl radical and a hydroxybenzyl radical, and the benzoyl radical subsequently undergoes a hydrogen atom transfer (HAT) process to generate the substrate radical. Based on this, a similar mechanism was proposed (Scheme 6). Upon visible light irradiation, the deprotonated **cat. 1** was activated to its excited state **cat. 1\***. **Cat. 1\*** interacts with the ground state **cat. 1**, furnishing the benzoyl radical **cat. 1'** and the hydroxybenzyl radical **cat. 1''**. The benzoyl radical **cat. 1'** then undergoes a HAT process with SPO **1** to generate the phosphonyl radical **I** and reform deprotonated **cat. 1**. Radical **I** undergoes an anti-Markovnikov addition with alkene **2**, generating radical **II**. Radical **II** abstracts the H radical from the hydroxybenzyl radical **cat. 1''**, producing the product **3** and reforming deprotonated **cat. 1**.<sup>30</sup> The base is proposed to be used for not only deprotonating the catalyst, but also facilitating the HAT processes.

## Conclusions

In conclusion, a visible light induced hydrophosphinylation of unactivated alkenes catalyzed by deprotonated salicylaldehyde is presented. This reaction has two advantages: low energy excitation (visible light: blue LED, 30 W) and a cheap catalyst source (salicylaldehyde: 55.0 CNY per 100 g, reagent grade 98%, from the company Energy Chemical). The reactions are easily performed in water and under an air atmosphere, and the products are produced in generally high yields. Better results can be obtained when the reaction is performed on a larger scale which further shows the potential utility of this methodology in industry. Based on the experimental results,

calculation studies and previous research, photoredox and EnT processes are excluded, and HAT activations are proposed for the mechanism.

## Conflicts of interest

There are no conflicts to declare.

## Acknowledgements

We thank the National Natural Science Foundation of China (Grant Nos. 21901177, 21572218 and 21772135) for financial support.

## Notes and references

- 1 For a recent book, see: *Organophosphorus Chemistry: From Molecules to Applications*, ed. V. Iaroshenko, Wiley-VCH, Verlag GmbH & Co. KGaA, 2019.
- 2 For selected reviews, see: (a) L. Albrecht, A. Albrecht, H. Krawczyk and K. A. Jørgensen, *Chem. – Eur. J.*, 2010, **16**, 28; (b) F. M. J. Tappe, V. T. Trepohl and M. Oestreich, *Synthesis*, 2010, 3037; (c) V. Koshti, S. Gaikwad and S. H. C. Chikkali, *Chem. Rev.*, 2014, **265**, 52; (d) J. Montchamp, *Acc. Chem. Res.*, 2014, **47**, 77; (e) X.-Q. Pan, J.-P. Zou, W.-B. Yi and W. Zhang, *Tetrahedron*, 2015, **71**, 7481; (f) L. Chen and Y.-X. Zou, *Org. Biomol. Chem.*, 2018, **16**, 7544; (g) S. Lemouzy, L. Giordano, D. Héroult and G. Buono, *Eur. J. Org. Chem.*, 2020, 3351.
- 3 (a) L. Coudray and J. Montchamp, *Eur. J. Org. Chem.*, 2008, 3601; (b) S. F. Malysheva, N. K. Gusarova, A. V. Artem'ev, N. A. Belogorlova, A. I. Albanov, T. N. Borodina, V. I. Smirnov and B. A. Trofimov, *Eur. J. Org. Chem.*, 2014, 2516; (c) Z. Li and W. Duan, *Chin. J. Org. Chem.*, 2016, **36**, 1805; (d) N. K. Gusarova, N. A. Chernysheva and B. A. Trofimov, *Synthesis*, 2017, **49**, 4783; (e) S.-Z. Nie, R. T. Favison and V. M. Dong, *J. Am. Chem. Soc.*, 2018, **140**, 16450; (f) Y. A. Rina and J. A. R. Schmidt, *Organometallics*, 2019, **38**, 4261; (g) S. Kawaguchi, Y. Yanamoto and A. Ogawa, *Mendeleev Commun.*, 2020, **30**, 129.
- 4 (a) S. Deprèle and J. Montchamp, *J. Am. Chem. Soc.*, 2002, **124**, 9386; (b) P. Ribière, K. Bravo-Altamirano, M. I. Antczak, J. D. Hawkins and J. Montchamp, *J. Org. Chem.*, 2005, **70**, 4064; (c) A. N. Reznikov and N. K. Skvortsov, *Russ. J. Gen. Chem.*, 2007, **77**, 1170; (d) K. Bravo-Altamirano, L. Coudray, E. L. Deal and J. Montchamp, *Org. Biomol. Chem.*, 2010, **8**, 5541; (e) C. Petit, F. Fécourt and J. Montchamp, *Adv. Synth. Catal.*, 2011, **353**, 1883; (f) S. Ortal, H. C. Fisher and J. Montchamp, *J. Org. Chem.*, 2013, **78**, 6599; (g) L.-B. Han, F. Mirzaei, C.-Q. Zhao and M. Tanaka, *J. Am. Chem. Soc.*, 2000, **122**, 5407; (h) C.-Q. Zhao, L.-B. Han and M. Tanaka, *Organometallics*, 2000, **19**, 4196; (i) F. Mirzaei, L.-B. Han and M. Tanaka, *Tetrahedron Lett.*, 2001, **42**, 297; (j) Q. Xu

- and L.-B. Han, *Org. Lett.*, 2006, **8**, 2099; (k) Q. Xu and L.-B. Han, *J. Organomet. Chem.*, 2011, **696**, 130.
- 5 (a) H. R. Hays, *J. Org. Chem.*, 1968, **33**, 3690; (b) P. Rey, J. Taillades, J. C. Rossi and G. Gros, *Tetrahedron Lett.*, 2003, **44**, 6169; (c) D. H. Cho and D. O. Jang, *Synlett*, 2005, 59; (d) L.-B. Han and C.-Q. Zhao, *J. Org. Chem.*, 2005, **70**, 10121; (e) A. F. Parsons, D. J. Sharpe and P. Taylor, *Synlett*, 2005, 2981; (f) M. I. Antczak and J. Montchamp, *Synthesis*, 2006, 3080; (g) H. C. Fisher, O. Berger, F. Gelat and J. Montchamp, *Adv. Synth. Catal.*, 2014, **356**, 1199; (h) S.-F. Zhou, D.-P. Li, K. Liu, J.-P. Zou and O. T. Asekun, *J. Org. Chem.*, 2015, **80**, 1214; (i) Z. Li, F. Fan, Z. Zhang, Y. Xiao, D. Liu and Z.-Q. Liu, *RSC Adv.*, 2015, **5**, 27853; (j) G.-Y. Zhang, C.-K. Li, D.-P. Li, R.-S. Zeng, A. Shoberu and J.-P. Zou, *Tetrahedron*, 2016, **72**, 2972; (k) L. Mao, Y. Li and S. Yang, *Chin. J. Chem.*, 2017, **35**, 316; (l) P.-Z. Zhang, L. Zhang, J.-A. Li, A. Shoberu, J.-P. Zou and W. Zhang, *Org. Lett.*, 2017, **19**, 5567; (m) N. Wang, L. Ye, Z.-L. Li, L. Li, Z. Li, H.-X. Zhang, Z. Guo, Q.-S. Gu and X.-Y. Liu, *Org. Chem. Front.*, 2018, **5**, 2810.
- 6 (a) C. M. Jessop, A. F. Parsons, A. Routledge and D. J. Irvine, *Eur. J. Org. Chem.*, 2006, 1547; (b) P. Troupa, G. Katsioulari and S. Vassiliou, *Synlett*, 2015, **26**, 2714.
- 7 (a) T. Hirai and L.-B. Han, *Org. Lett.*, 2007, **9**, 53; (b) Z. Huang, W. Liu, S. Li, Y. Yang, S. Guo and H. Cai, *Synlett*, 2020, **31**, 1295.
- 8 (a) A. N. Reznikov and N. K. Skvortsov, *Russ. J. Gen. Chem.*, 2008, **78**, 320; (b) S. Kawaguchi, A. Nomoto, M. Sonoda and A. Ogawa, *Tetrahedron Lett.*, 2009, **50**, 624; (c) P.-Y. Geant, J.-P. Uttaro, S. Peyrottes and C. Mathé, *Eur. J. Org. Chem.*, 2017, 3850.
- 9 For selected reviews, see: (a) J. M. R. Narayanam and C. R. J. Stephenson, *Chem. Soc. Rev.*, 2011, **40**, 102; (b) J. Xuan and W.-J. Xiao, *Angew. Chem., Int. Ed.*, 2012, **51**, 6828; (c) C. K. Prier, D. A. Rankic and D. W. C. MacMillan, *Chem. Rev.*, 2013, **113**, 5322; (d) C. Wang and Z. Lu, *Org. Chem. Front.*, 2015, **2**, 179; (e) J. Xuan, Z.-G. Zhang and W.-J. Xiao, *Angew. Chem., Int. Ed.*, 2015, **54**, 15632; (f) K. L. Skubi, T. R. Blum and T. P. Yoon, *Chem. Rev.*, 2016, **116**, 10035; (g) N. A. Romero and D. A. Nicewicz, *Chem. Rev.*, 2016, **116**, 10075; (h) I. K. Sideri, E. Voutyritsa and C. G. Kokotos, *Org. Biomol. Chem.*, 2018, **16**, 4596; (i) F. Strieth-Kalthoff, M. J. James, M. Teders, L. Pitzer and F. Glorius, *Chem. Soc. Rev.*, 2018, **47**, 7190; (j) *Visible Light Photocatalysis in Organic Chemistry*, ed. C. R. J. Stephenson, T. P. Yoon and D. W. C. MacMillan, Wiley-VCH, Weinheim, 2018; (k) Q.-Q. Zhou, Y.-Q. Zou, L.-Q. Lu and W.-J. Xiao, *Angew. Chem.*, 2019, **58**, 1586; (l) X.-Y. Yu, Q.-Q. Zhao, J. Chen, W.-J. Xiao and J.-R. Chen, *Acc. Chem. Res.*, 2020, **53**, 1066.
- 10 (a) W. Yoo and S. Kobayashi, *Green Chem.*, 2013, **15**, 1844; (b) G. Fausti, F. Morlet-Savary, J. Lalevée, A. Gaumont and S. Lakhdar, *Chem. – Eur. J.*, 2017, **23**, 2144. For a review, see: (c) B.-G. Cai, J. Xuan and W.-J. Xiao, *Sci. Bull.*, 2019, **64**, 337.
- 11 For similar results, see: Y. Shi, R. Chen, K. Guo, F. Meng, S. Cao, C. Gu and Y. Zhu, *Tetrahedron Lett.*, 2018, **59**, 2062.
- 12 H. Wang, Y. Li, Z. Tang, S. Wang, H. Zhang, H. Cong and A. Lei, *ACS Catal.*, 2018, **8**, 10599.
- 13 M.-J. Bu, G.-P. Lu and C. Cai, *Catal. Sci. Technol.*, 2016, **6**, 413.
- 14 (a) D. Liu, J.-Q. Chen, X.-Z. Wang and P.-F. Xu, *Adv. Synth. Catal.*, 2017, **359**, 2773; (b) X.-C. Liu, K. Sun, X.-L. Chen, W.-F. Wang, Y. Liu, Q.-L. Li, Y.-Y. Peng, L.-B. Qu and B. Yu, *Adv. Synth. Catal.*, 2019, **361**, 3712; (c) R. Gorre, D. Enagandhula, S. Balasubramanian and S. M. Akondi, *Org. Biomol. Chem.*, 2020, **18**, 1354.
- 15 H.-F. Qian, C.-K. Li, Z.-H. Zhou, Z.-K. Tao, A. Shoberu and J.-P. Zou, *Org. Lett.*, 2018, **20**, 5947.
- 16 Y. Yin, W.-Z. Weng, J.-G. Sun and B. Zhang, *Org. Biomol. Chem.*, 2018, **16**, 2356.
- 17 Q. Fu, Z.-Y. Bo, J.-H. Ye, T. Ju, H. Huang, L.-L. Liao and D.-G. Yu, *Nat. Commun.*, 2019, **10**, 3592.
- 18 For aldehyde catalysis in photochemical reactions, see: (a) M. A. Theodoropoulou, N. F. Nikitas and C. G. Kokotos, *Beilstein J. Org. Chem.*, 2020, **16**, 833; (b) Z. Yuan, J. Liao, H. Jiang, P. Cao and Y. Li, *RSC Adv.*, 2020, **10**, 35433.
- 19 (a) E. Arceo, E. Montroni and P. Melchiorre, *Angew. Chem., Int. Ed.*, 2014, **53**, 12064; (b) I. K. Sideri, E. Voutyritsa and C. G. Kokotos, *ChemSusChem*, 2019, **12**, 4194; (c) V. Pirenne, I. Traboulsi, L. Rouvière, J. Lusseau, S. Massip, D. M. Bassani, F. Robert and Y. Landais, *Org. Lett.*, 2020, **22**, 575; (d) T. Yajima, M. Murase and Y. Ofuji, *Eur. J. Org. Chem.*, 2020, 3808; (e) N. F. Nikitas, M. A. Theodoropoulou and C. G. Kokotos, *Eur. J. Org. Chem.*, 2021, 1168.
- 20 For a recent example of changing the light absorbing wavelength of a simple catalyst by adjusting the substituents, see: L. D. Elliott, S. Kayal, M. W. George and K. Booker-Milburn, *J. Am. Chem. Soc.*, 2020, **142**, 14947.
- 21 Y.-J. Zhuang, J.-P. Qu and Y.-B. Kang, *J. Org. Chem.*, 2020, **85**, 4386.
- 22 See the ESI† for detailed reaction condition optimization.
- 23 For selected reviews, see: (a) D. E. Metzler, M. Ikawa and E. E. Snell, *J. Am. Chem. Soc.*, 1954, **76**, 648; (b) R. A. John, *Biochim. Biophys. Acta*, 1995, **1248**, 81; (c) J. Liang, Q. Han, Y. Tan, H. Ding and J. Li, *Front. Mol. Biosci.*, 2019, **6**, 1.
- 24 For recent applications of alkyl(aryl)phosphine oxide in transition metal mediated phosphinylation reaction, see: (a) R. Beaud, R. J. Phipps and M. J. Gaunt, *J. Am. Chem. Soc.*, 2016, **138**, 13183; (b) X.-T. Liu, Y.-Q. Zhang, X.-Y. Han, S.-P. Sun and Q.-W. Zhang, *J. Am. Chem. Soc.*, 2019, **141**, 16584.
- 25 A. N. Yarkevich, L. N. Petrova and S. O. Bachurin, *Russ. J. Gen. Chem.*, 2012, **82**, 1659.
- 26 For alkynes with the less hindered R<sup>5</sup> group, a (Z)-isomer of a σ-bent vinyl radical intermediate would be dominant, leading to cis-addition. For alkynes with the more hindered R<sup>5</sup> group, a π-linear vinyl radical or an (E)-isomer of a σ-bent vinyl radical intermediate would be dominant due to the steric impact, leading to trans-addition. See the follow-

- ing references and referred articles: (a) K. Griesbaum, *Angew. Chem., Int. Ed. Engl.*, 1970, **9**, 273; (b) C. Galli, A. Guarnieri, H. Koch, P. Mencarelli and Z. Rappoport, *J. Org. Chem.*, 1997, **62**, 4072; (c) T. P. M. Goumans, K. Alem and G. Lodder, *Eur. J. Org. Chem.*, 2008, 435.
- 27 Y. Wang, H. Jiang, J.-J. Tian and J.-B. He, *Electrochim. Acta*, 2014, **125**, 133. The study showed that the anodic peak potential remained relatively constant (around 0.8 V vs. Ag/AgCl electrode; Ag/AgCl electrode: 0.195 V vs. SHE) when the pH value was greater than 9.2. (SHE refers to standard hydrogen electrode).
- 28 In ref. 10a, the oxidation potential of **1a** was assumed to be similar to that of triphenylphosphine (1.0 V vs. SCE).
- 29 The absolute fluorescence quantum yield of salicylaldehyde was measured at 417 nm: 2.10%. Sample: salicylaldehyde ( $10^{-4}$  mol L $^{-1}$ ) and Na $_2$ CO $_3$  ( $10^{-2}$  mol L $^{-1}$ ) in distilled water. See the ESI† for more details.
- 30 A similar HAT process is found using aromatic ketones as photocatalysts: (a) T. Yamashita, M. Yasuda, M. Watanabe, R. Kojima, K. Tanabe and K. Shima, *J. Org. Chem.*, 1996, **61**, 6438; (b) S. Bertrand, N. Hoffmann, S. Humbel and J. P. Pete, *J. Org. Chem.*, 2000, **65**, 8690.